2. N. Liang, J. R. Miller, G. L. Closs, *ibid.* **112**, 5353 (1990), and references therein.
3. C. E. D. Chidsey, C. R. Bertozzi, T. M. Putvinski, A. M. Mujsce, *ibid.*, p. 4301.
4. R. G. Nuzzo and D. L. Allara, *ibid.* **105**, 4481 (1983).
5. M. D. Porter, T. B. Bright, D. L. Allara, C. E. D. Chidsey, *ibid.* **109**, 3559 (1987).
6. C. D. Bain *et al.*, *ibid.* **111**, 321 (1989).
7. C. E. D. Chidsey and D. N. Loiacono, *Langmuir* 6, 682 (1990).
8. L. Strong and G. M. Whitesides, *ibid.* **4**, 546 (1988).
9. C. E. D. Chidsey, G.-Y. Liu, P. Rowntree, G. Scoles, *J. Chem. Phys.* **91**, 4421 (1989).
10. R. G. Nuzzo, L. H. Dubois, D. L. Allara, *J. Am. Chem. Soc.* **112**, 558 (1990).
11. R. G. Nuzzo, E. M. Korenic, L. H. Dubois, *J. Chem. Phys.* **93**, 767 (1990).
12. A. J. Bard and L. R. Faulkner, *Electrochemical Methods: Fundamentals and Applications* (Wiley, New York, 1980).
13. Due to the large separation, the interfacial potential gradient is calculated to occur almost entirely between the electroactive group and the electrode. As a result, no double-layer corrections are needed in the kinetic analysis.
14. The intrinsic time constant of the cell and the uncompensated cell resistance are measured to be 3 μs and 4 ohms, respectively, by an ac impedance technique, ruling out resistive artifacts in Figs. 2 to 4.
15. E. Laviron, *J. Electroanal. Chem.* **101**, 19 (1979).
16. R. A. Marcus, *J. Chem. Phys.* **43**, 679 (1965).
17. V. G. Levich, in *Advances in Electrochemistry and Electrochemical Engineering*, P. Delahay, Ed. (Interscience, New York, NY, 1966), vol. 4, pp. 249.
18. J. Ulstrup and J. Jortner, *J. Chem. Phys.* **63**, 4358 (1975).
19. M. D. Newton and N. Sutin, *Annu. Rev. Phys. Chem.* **35**, 437 (1984).
20. M. A. Ratner, *J. Phys. Chem.* **94**, 4877 (1990), and references therein.
21. W. Schmickler, *J. Electroanal. Chem.* **204**, 31 (1986); J. D. Morgan and P. G. Wolynes, *J. Phys. Chem.* **91**, 874 (1987); L. D. Zusman, *Chem. Phys.* **112**, 53 (1987); A. K. Mishra and S. K. Rangarajan, *J. Phys. Chem.* **91**, 3417 (1987); K. L. Sebastian, *J. Chem. Phys.* **90**, 5056 (1989).
22. T. Gennett, D. F. Milner, M. J. Weaver, *J. Phys. Chem.* **89**, 2787 (1985).
23. If a tunneling decay length of 1 Å is assumed, then the number of metal atoms within tunneling distance is of order 10. If each metal atom contributes one state to a band of order 10 eV wide, then the effective density of states ρ is ~1 eV^{-1}. With $\upsilon\rho \approx 10^{-5}$ $s^{-1}eV^{-1}$, the effective per state υ, is ~10^{-5} s^{-1}; υ is given by (*24*)

$$\upsilon = \frac{\sqrt{\pi}}{\hbar}\frac{|V|^2}{\sqrt{\lambda k_B T}}$$

where ħ is Planck's constant over 2π. The resulting electronic coupling V is of order 10^{-6} eV (10^{-2} cm^{-1}).
24. N. R. Kestner, J. Logan, J. Jortner, *J. Phys. Chem.* **78**, 2148 (1974); B. S. Brunschwig, J. Logan, M. D. Newton, N. Sutin, *J. Am. Chem. Soc.* **102**, 5798 (1980); R. A. Marcus and P. Siders, *J. Phys. Chem.* **86**, 622 (1982).
25. C. E. D. Chidsey and T. M. Putvinski, unpublished results.
26. The solvent reorganization energy is calculated from the dielectric continuum model (*16*) for ferrocene with a 3.8 Å solvation radius (*22*) in water 20 Å from a metallic electrode. The calculated value may be high because it assumes that the ion is bathed in an infinite bath of water, whereas the real ion is flanked by a 20-Å–thick sheet of hydrocarbon.

30 August 1990; accepted 12 November 1990

Charge Separation in a Reaction Center Incorporating Bacteriochlorophyll for Photoactive Bacteriopheophytin

CHRISTINE KIRMAIER, DALE GAUL, RANDY DEBEY, DEWEY HOLTEN, CRAIG C. SCHENCK

Site-directed mutagenic replacement of M subunit Leu^{214} by His in the photosynthetic reaction center (RC) from *Rhodobacter sphaeroides* results in incorporation of a bacteriochlorophyll molecule (BChl) in place of the native bacteriopheophytin (BPh) electron acceptor. Evidence supporting this conclusion includes the ground-state absorption spectrum of the (M)L214H mutant, pigment and metal analyses, and time-resolved optical experiments. The genetically modified RC supports transmembrane charge separation from the photoexcited BChl dimer to the primary quinone through the new BChl molecule, but with a reduced quantum yield of 60 percent (compared to 100 percent in wild-type RCs). These results have important implications for the mechanism of charge separation in the RC, and rationalize the choice of (bacterio)pheophytins as electron acceptors in a variety of photosynthetic systems.

CHARGE SEPARATION IN THE RC complex from photosynthetic bacteria (Fig. 1) involves the reduction of the BPh electron acceptor associated with the L polypeptide within a few picoseconds of excitation of the BChl dimer, P. Subsequently, the BPh_L anion transfers an electron in a few hundred picoseconds to the primary quinone (Q_A), forming $P^+Q_A^-$. In this way, charges are stably separated across the membrane with unity quantum yield, even at cryogenic temperatures (*1*). The crystal structures of RCs from two bacterial species have revealed this protein complex to be highly symmetric: BPh_L, the $BChl_L$ monomer, Q_A, and the L polypeptide folding pattern obey approximate C_2 symmetry with respect to BPh_M, $BChl_M$, Q_B, and the folding of the M polypeptide (*2–4*). Both $BChl_L$ and $BChl_M$ are in van der Waals contact with a BChl ring of P and ~5 Å from their neighboring BPh_L and BPh_M, respectively. Determination of the role of $BChl_L$ in the initial reduction of BPh_L and elucidation of the molecular factors responsible for the unidirectional asymmetry of charge separation to BPh_L are critical issues in current efforts toward a microscopic understanding of light-induced charge separation in photosynthetic RCs.

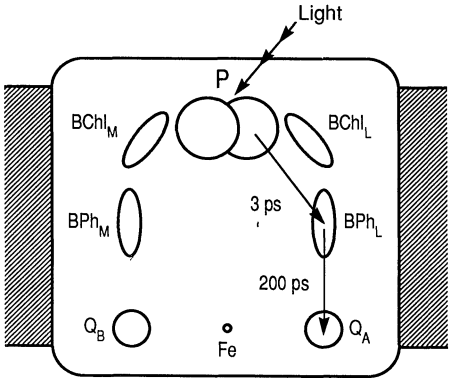

Fig. 1. Schematic representation of the cofactor arrangement in the bacterial reaction center. Symbols are defined in the text.

A His residue is located adjacent to the Mg^{2+} of each of the four BChls. The crystal structures have generally identified these His residues to be ligands to the Mg^{2+} ions, although some exceptions to this have been reported (*3*). The BPhs lack a central Mg^{2+} ion and do not have metal-coordinating ligands from the protein over the macrocycle centers. A conserved Leu on the M subunit (residue 214 in *Rb. sphaeroides*) is located roughly over the center of the BPh_L chromophore (*4*). We have replaced this Leu with the potential metal-coordinating residue His in a *Rb. sphaeroides* stain derived from wild-type (wt) WS8 (*5*).

Comparison of the ground-state absorption spectrum of RCs isolated from the (M)L214H mutant (Fig. 2, dashed) with the spectrum of wt RCs (solid) reveals that while the 865-nm band of P is unperturbed, several other key absorption bands are altered. In the difference spectrum, (M)L214H RCs are distinguished from wt by the appearance of a Q_Y band near 785 nm, stronger Q_X absorption at 600 nm, and less absorption in the BPh bands near 760 and 545 nm. These changes are consistent with the replacement of BPh_L with BChl. In this regard, all available spectroscopic information on tetrapyrroles makes it difficult to reconcile the mutation-induced spectral changes as representing merely a shift of the BPh_L Q_X band from 545 to 600 nm due to

C. Kirmaier and D. Holten, Department of Chemistry, Washington University, St. Louis, MO 63130.
D. Gaul, R. DeBey, C.C. Schenck, Department of Biochemistry, Colorado State University, Fort Collins, CO 80523.

the presence of a histidine over the center of the metal-free chromophore (*6–8*).

The results of quantitative assays of the pigment content and stoichiometry given in Table 1 indicate that the majority of the (M)L214H RCs have incorporated a BChl molecule, which we designate β_L, in place of the native BPh_L electron carrier. Note that the most straightforward assay, the BChl/BPh pigment ratio, indicates that at least 85% of the (M)L214H RCs contain five BChls and one BPh. Such an altered pigment content is consistent with the ground-state absorption spectrum and the time-resolved absorption measurements described below. X-ray diffraction data on single crystals of the (M)L214H mutant indicate a significant electron density at the center of the tetrapyrrole ring at the BPh_L site, consistent with the presence of a Mg atom (*9*). Our finding that placement of a His over the center of a BPh promotes incorporation of BChl is complementary to the observation that removal of the His associated with the central Mg^{2+} of either BChl of P results in the incorporation of BPh into the appropriate binding site (*10–12*).

The (M)L214H RC can support the overall primary charge-separation process yielding $P^+Q_A^-$, in agreement with the observation that the mutant grows photoheterotrophically. The transient absorption spectrum observed 2 ns after a 150-fs excitation flash (*13*) has features expected for this state, including bleaching of the 865-nm band of P and a bandshift-like feature centered near 800 nm (Fig. 3). The P-band bleaching decays with a time constant on the order of 100 ms, characteristic of the $P^+Q_A^-$ charge-recombination reaction in wt RCs (*14*). The yield of $P^+Q_A^-$ is ~60%, compared to 100% in wt RCs, as indicated in Fig. 3 by an initial 40% recovery of the 865-nm bleaching of P between the two early-time spectra (400 fs and 30 ps) and the 2-ns $P^+Q_A^-$ spectrum. The finding that charge separation takes place in (M)L214H RCs is remarkable in view of the replacement of the native BPh_L electron carrier with BChl, a pigment with significantly different redox properties in vitro (*7, 15*).

A description of the electron transfer events in (M)L214H RCs leading to this 60% yield of $P^+Q_A^-$ is obtained from the data in Figs. 4 and 5, which compare spectra for wt and (M)L214H RCs acquired under identical conditions on samples having the same concentration. (Note that the amplitudes of the absorption changes in the two samples thus can be compared to give a quantitative assay of the photochemistry in (M)L214H RCs.) The spectrum of P* (the excited primary electron donor) at 400 fs is essentially identical in wt and (M)L214H RCs, showing the characteristic flat and featureless absorption between 500 and 800 nm, broken by bleaching of the Q_X band of P near 600 nm (Figs. 4 and 5A). The P* spectrum in (M)L214H RCs is further characterized by bleaching of the 865-nm band of P superimposed on the P* stimulated emission band between 870 and 1000 nm, as shown in the 400-fs spectrum in Fig. 3. (An identical P-bleaching and stimulated emission spectrum is found for wt RCs.) The lifetime of P* in (M)L214H RCs (measured by decay of stimulated emission) is 6.4 ± 0.8 ps, which is about a factor of 2 longer than the lifetime of 3.5 ± 0.3 ps observed in wt RCs and associated with P* → $P^+BPh_L^-$.

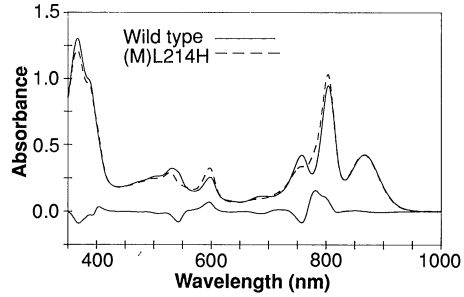

Fig. 2. The upper traces compare the 295-K absorption spectra of wt (——) and (M)L214H (- - - -) RCs in 10 mM tris, pH8, 0.05% LDAO buffer. The spectra have been normalized at the 865 nm absorption peak of P. In wt RCs absorption bands are assigned basically as follows: 865 nm, the long-wavelength transition of P; 805 and 760 nm, the Q_Y bands of the monomeric BChls and BPhs, respectively; 600 nm, the Q_X transitions of all four BChls; 530 and 545 nm, the Q_X bands of BPh_M and BPh_L, respectively, which partially overlap at 295 K. (The single carotenoid also contributes in the 450- to 550-nm region.) Subtraction of the wt spectrum from that of (M)L214H RCs gives the difference spectrum shown as the lower trace, which is indicative of reduced BPh and increased BChl content in the mutant (see text).

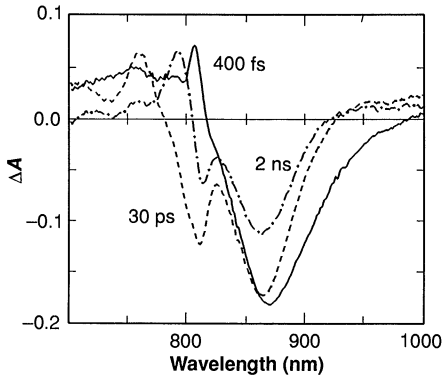

Fig. 3. Transient absorption difference spectra of (M)L214H RCs observed 0.4 ps (——), 30 ps (- - - -), and 2 ns (—·—) after a 150-fs excitation flash at 870 nm. Other conditions as in (*13*).

Table 1. RC Content and stoichiometries. The (M)L214H RCs used in these assays (as well as in the time-resolved experiments) had $A_{280}/A_{800} \simeq 1.06$. ($A_x$ is the absorbance at the peak of the bands near 280 and 800 nm.) The results and standard deviations from four to six determinations of each quantity are shown. The numbers in square brackets are the known values for the pigment content of wt RCs. The numbers in parentheses are the values expected if a BPh is replaced by BChl in the mutant.

	Mg^{2+}/ RC*	(Pigments)/ RC†	BChl/ BPh†
Wild type	3.9 ± 0.4 [4]	5.6 ± 0.4 [6]	1.8 ± 0.2 [2]
(M)L214H	4.6 ± 0.4 (5)	5.6 ± 0.4 (6)	4.5 ± 0.5 (5)

*Determined by inductively coupled plasma atomic emission spectroscopy (*37*) by comparison with standard solutions of Mg^{2+} salts in detergent buffer. The Mg^{2+} stoichiometry (requiring knowledge of the RC concentration of the samples) was based on the protein absorption at 280 nm and made use of the extinction coefficient for wt RCs (which had $A_{280}/A_{800} \simeq 1.21$). †Determined by extraction of the pigments into acetone:methanol (7:2) (*8, 11*). The BChl/BPh pigment ratio assay is independent of assumptions about extinction coefficients in vivo, whereas the pigments/RC assay requires knowledge of the RC concentration (which was determined from the absorbance at 865 nm utilizing the 865-nm extinction coefficient for wt RCs). The BChl/BPh ratio of 4.5 corresponds to 85% of the (M)L214H RCs containing five BChls and one BPh. An upward correction of the ratio by 10% (the BChl/BPh ratio for wt RCs is ~10% low) would indicate that a BChl has replaced a BPh in essentially all of the (M)L214H RCs.

The spectral region between 500 and 700 nm is particularly useful for identifying the transient state formed following P* decay; this region encompasses the Q_X bands of the chromophores (500 to 600 nm) and the broad yet pronounced absorption bands of both BPh and BChl anions (600 to 700 nm). The spectrum of $P^+BPh_L^-$ at 15 ps in wt RCs (Fig. 4A) shows bleaching of the 545-nm Q_X band of BPh_L and the characteristic broad 665-nm BPh_L anion band. These features develop with time constants of ~3.5 ps, in agreement with the P* stimulated emission decay time. Bleaching of the Q_X band of P near 600 nm is the same in wt RCs for states P* and $P^+BPh_L^-$, as expected.

A novel intermediate state forms as P* decays in (M)L214H RCs (Fig. 4B). The 30-ps spectrum in the mutant has a broad absorption band centered near 690 nm that develops with a time constant (6.5 ± 1.5 ps) which is the same within experimental error as the P* stimulated emission lifetime. During this time an increase in the bleaching in the BChl Q_X region near 600 nm develops. These spectral features are notably different from those due to reduction of BPh_L in wt RCs and are consistent with the reduction of a BChl. Hence, we believe that P* decays in (M)L214H RCs by electron transfer to β_L to form $P^+\beta_L^-$. The formation of a BChl

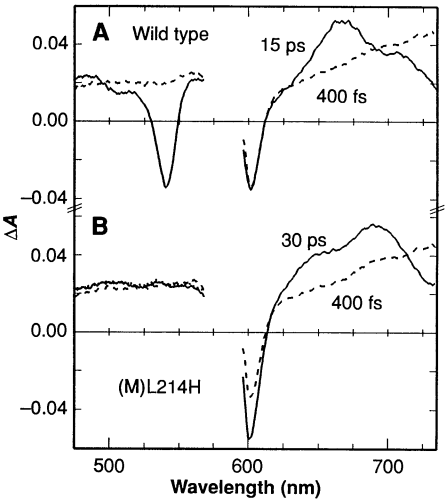

Fig. 4. Comparison of the visible-region transient spectra observed under identical experimental conditions on wt (**A**) and (M)L214H (**B**) RC samples of the same concentration (as judged by their 865-nm absorption). In wt RCs the 400-fs spectrum (- - - -) and 15-ps spectra (——) are associated with P* and $P^+BPh_L^-$, respectively. In (M)L214H RCs an identical P* spectrum is observed at 400 fs (- - -). The 30-ps spectrum (——) for (M)L214H has features that are much different and which may be ascribed to reduction of a BChl (β_L); this spectrum of $P^+\beta_L^-$ is equivalent to the 15-ps spectrum of $P^+BPh_L^-$ in wt RCs in the sense that both were measured at about five P* lifetimes. In (B) a 15-ps spectrum (•••) is also plotted between 480 and 570 nm (essentially coincident with the 400-fs and 30-ps spectra); the wt spectra show maximal 540-nm bleaching of BPh_L at this time. Other conditions as in (*13*).

anion is supported by the observation that the anion band of BChl in vitro is red-shifted from that of BPh (*7*). Further, one expects that the reduction of a BChl would give rise to bleaching near 600 nm in addition to the bleaching of the Q_X band of P. State $P^+\beta_L^-$ appears to form with the same high quantum yield (~1.0) as $P^+BPh_L^-$ in wt RCs. This high yield is determined from two observations: (i) there is essentially no decay of bleaching in the 865-nm band of P (no ground-state recovery) during the P* lifetime (compare 400-fs and 30-ps spectra in Fig. 3); and (ii) the amplitude of the 690-nm anion band of $P^+\beta_L^-$ in the mutant is comparable to that of the 665-nm anion band of $P^+BPh_L^-$ in wt RCs (Fig. 4). The anion bands of BChl and BPh in vitro also have comparable extinction coefficients (*7*). The second point also indicates that we are witnessing photochemistry in the majority (essentially all) of the RCs and not just some small subpopulation.

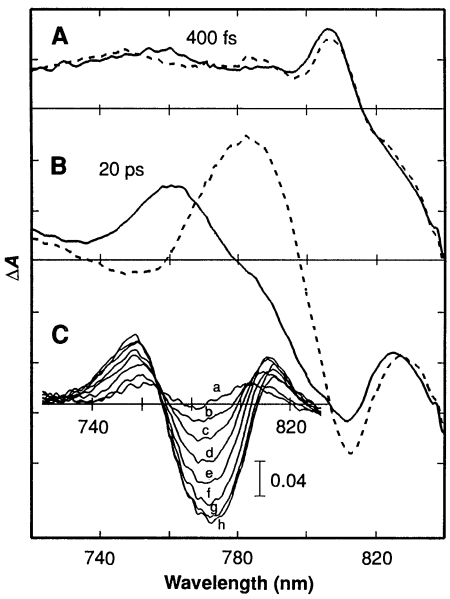

Fig. 5. Transient absorption changes in the Q_Y region for wt (- - - -) and (M)L214H (——) RCs. (**A**) Comparison of the 400-fs P* spectra, which are the same within experimental error in the two RCs. (**B**) Comparison of the 20-ps spectra of the intermediate states between P* and $P^+Q_A^-$: $P^+BPh_L^-$ in wt RCs, and the state identified as $P^+\beta_L^-$ in (M)L214H RCs. The difference between the spectra in (A) and (B) (the absorbance changes for wt RCs subtracted from those for (M)L214H RCs) are shown (**C**) as traces (a) and (h), respectively. The other traces in (C) are similar subtractions of the (M)L214H and wt spectra at (b) 1.1, (c) 1.8, (d) 3.3, (e) 4.8, (f) 7.9, and (g) 14 ps. Other conditions as in (*13*).

The spectra of (M)L214H RCs are devoid of bleaching in the region between 500 and 570 nm throughout the time course from 400 fs to 2 ns (Fig. 4B). This key result first shows that there is no evidence for photochemically active BPh_L (the native acceptor) in the mutant since there is no bleaching near 545 nm (≤10% active BPh_L present based on the signal-to-noise ratio in Fig. 4B). This finding is consistent with the ground-state absorption spectrum, pigment analysis, and transient absorption data at longer wavelengths (see above). The second important implication of this result is that there is no evidence for electron transfer to the symmetry-related BPh_M molecule as would be evidenced by bleaching of its 530-nm Q_X band.

The data in Fig. 5 more directly implicate β_L as the reduced electron carrier between P* and $P^+Q_A^-$. As in the Q_X and anion regions, the 20-ps spectra between 720 and 840 nm are very different for $P^+\beta_L^-$ in (M)L214H RCs (Fig. 5B, solid) and $P^+BPh_L^-$ in wt RCs (dashed). The difference between these two spectra is given as spectrum h in Fig. 5C. Spectrum a is the difference between the two P* spectra in part A, while spectra b through g show the difference between the mutant and wt transient spectra at several intervening times spanning the P* lifetime. This series of $\Delta\Delta A$ spectra show that a net bleaching near 785 nm develops as P* decays. The wavelength of this net bleaching closely matches the position of the new Q_Y ground-state absorption in (M)L214H RCs (Fig. 2) and can be associated with reduction of β_L. Since $BChl_L$ could contribute to the 785-nm absorption due to exciton coupling with β_L, it is possible that some electron density in β_L^- is shared with $BChl_L$. However, if the state present after P* decay were predominately $P^+BChl_L^-$ (or $P^+BChl_M^-$), then we would have expected the main bleaching in Fig. 5C to occur near 800 to 810 nm.

It is in subsequent electron transfer, $P^+\beta_L^- \rightarrow P^+Q_A^-$, and not in the initial electron transfer from P*, that the reduction in quantum yield is observed. State $P^+\beta_L^-$ has a lifetime of 325 ± 25 ps as measured by decay of the 690-nm anion band; there is good agreement between this value and the 400 ± 75 ps measured for the 40% decay of bleaching of the 865-nm band of P (Fig. 3). Hence, $P^+\beta_L^-$ decays 60% by electron transfer to Q_A and 40% by return to the ground state during its ~350 ps lifetime. Reduction of Q_A (~350 ps/0.6 ≃ 600 ps) is about a factor of 3 slower than in wt RCs, while competing deactivation of $P^+\beta_L^-$ to the ground state (~350 ps/0.4 ≃ 900 ps) is more than a factor of 10 faster than charge recombination within $P^+BPh_L^-$ in wt RCs (*16*). Confirming the latter finding, the time constant for $P^+\beta_L^-$ decay to the ground state measured under conditions where electron transfer to Q_A is blocked is ~850 ps (*17*). An enhanced charge-recombination pathway competing effectively with electron transfer to Q_A is thus responsible for the reduced $P^+Q_A^-$ quantum yield in (M)L214H RCs.

One expects replacement of BPh_L with BChl (β_L) to raise the free energy (ΔG) of the radical pair ($P^+\beta_L^-$ versus $P^+BPh_L^-$) with respect to the ground state since BChl in vitro is harder to reduce than BPh by 200 to 300 meV (*7, 15*). To investigate this, the free energy of $P^+\beta_L^-$ with respect to P* was determined from the delayed fluorescence from P* at room temperature (*18*). [Steady-state measurements on (M)L214H RCs reveal an emission band centered near 915 nm similar to that found in wt RCs and ascribed to fluorescence from P*.] It is evident from Fig. 6A that a considerable fraction of the emission from the (M)L214H mutant is delayed compared to emission from wt RCs (which approximates the instrument response). The wt signal was used to deconvolve prompt from delayed components in the fluorescence of the mutant. The results (Fig. 6B) give the prompt component, a major delayed component (time constant τ

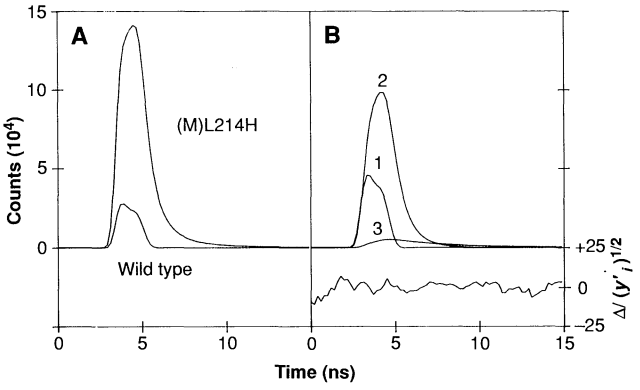

Fig. 6. (**A**) Observed time-resolved fluorescence at 920 nm from (M)L214H RCs (upper curve) and from wt RCs (lower curve), with the latter approximating the instrument response to a δ function excitation. (**B**) The deconvolved components (*18, 19*). A five-parameter fit with a prompt component (trace 1) and two delayed components (traces 2 and 3) was required to successfully model the data, as ascertained by the weighted residuals [(B), bottom and right-hand ordinate; see (*19*)]. Deconvolution parameters are described in the text.

= 0.7 ± 0.3 ns), and a minor delayed component (τ = 3.2 ± 1.0 ns) in the ratio of 1.7:4.8:0.6 compared to the integrated intensity of wt emission. (The minor component may represent trace impurity fluorophores.) If we use a simple two-state model, then the initial amplitude of the major delayed component indicates that $P^+\beta_L^-$ lies 75 ± 30 meV in free energy below P* in the mutant. This $-\Delta G°$ is considerably smaller than the 160-meV gap between P* and $P^+BPh_L^-$ in wt RCs (*19*). The ~85-meV difference between wt and (M)L214H RCs is smaller than expected based on solution redox potentials of BPh and BChl. This difference could reflect (i) structural or electrostatic protein perturbations holding the cofactor within a functional redox potential range, and (ii) mixing between $P^+\beta_L^-$ and a higher energy state such as $P^+BChl_L^-$.

The factor of 1.7 increased yield of the prompt fluorescence component in the mutant correlates well with the increased P* lifetime (6.5 versus 3.5 ps) in (M)L214H RCs relative to wt. In the simplest model, the time course of the delayed components should show kinetic equivalence with the states measured in absorption. The lifetime of the major delayed fluorescence component (0.7 ± 0.3 ns) agrees reasonably well with the radical-pair lifetime measured in transient absorption (0.35 ± 0.06 ns). The observed time constants in (M)L214H RCs vary with detection wavelength in the Q_Y region of the transient absorption spectra. (The values measured in the P* stimulated emission and 690-nm anion bands are roughly equal to the mean of a range of values obtained in the Q_Y region.) Similar results for both electron transfer from P* to BPh_L and from BPh_L^- to Q_A have been recently reported for wt *Rb. sphaeroides* R26 RCs and attributed to an inhomogeneous distribution of RCs, with each conformer reacting with slightly different rates (*20*). The different rates of electron transfer among the members of such a distribution may reflect in part differences in the energy of the radical-pair state in both wt and (M)L214H RCs. Thus a complete description of the delayed fluorescence may require a distribution of states weighted by the Boltzmann factor, although this should not qualitatively affect our conclusion that $-\Delta G°$ in the mutant is substantially smaller than in wt RCs.

A mechanistically important conclusion that can be drawn from our results is that the rate of electron transfer from P* to BPh_L (or β_L) depends rather weakly on the free energy gap; this rate changes by only a factor of 2 despite a large fractional change in $-\Delta G°$ from 160 meV in wt to ~75 meV in (M)L214H RCs. The weak $-\Delta G°$ dependence of this rate, evident here and in other recent work (*21, 22*), could reflect a shallow potential surface for P* with numerous coordinates available for passage to the radical-pair state involving weak coupling to many modes of the pigment-protein complex (*23–25*). An additional factor may be a very small pigment-protein reorganization energy λ, at least on the time scale of the initial reaction. Such constraints would temper the effect of a change in energetics on the Franck-Condon factor and help to explain why even for the very small $-\Delta G°$ in the mutant the initial reaction does not lie in the activated region where $-\Delta G° < \lambda$ (*26*). The activationless nature of this process in (M)L214H RCs follows from our observation that the P* lifetime at 5 K is ~2.5 ps.

Another consideration in understanding the mechanism of initial electron transfer is the role of the $BChl_L$ monomer. This issue is still being debated with respect to wt RCs, with two basic ideas receiving the most attention (*21, 27–31*): (i) a two-step process, $P^* \rightarrow P^+BChl_L^- \rightarrow P^+BPh_L^-$, wherein $P^+BChl_L^-$ is a true chemical intermediate and the second step is much faster than the first; and (ii) a superexchange mechanism in which $P^+BChl_L^-$ is not discretely populated but quantum mechanically mixes with P* and $P^+BPh_L^-$. A key issue is the energy of $P^+BChl_L^-$. There is little experimental information about the $P^+BChl_L^-$ energy, although some estimates and constraints have been discussed (*21, 28–31*). If $P^+BChl_L^-$ lies only slightly above P* (within ~kT), then a combined superexchange/thermally activated two-step mechanism could operate at 295 K with the former dominant at cryogenic temperatures (*31*). In considering a two-step mechanism, if $P^+BChl_L^-$ lies below P* in (M)L214H RCs, then our results show that the separation between these states must be less than ~75 meV. A 75-meV free energy gap is a very narrow window to accommodate two consecutive ultrafast activationless electron transfer processes and hence places even greater constraints on λ and the shapes of the relevant potential surfaces than in wt RCs. Additionally, in order for the two-step mechanism to be tenable in (M)L214H RCs, one must hypothesize that replacement of BPh_L with β_L affects the rate of electron transfer from P* to $BChl_L$.

The most dramatic difference in (M)L214H RCs is found in the increased rate of charge recombination ($P^+\beta_L^- \rightarrow P$) and the consequent decrease in the yield of $P^+Q_A^-$. Since it is difficult to see how an altered Franck-Condon factor could fully account for a greater than tenfold increase in the charge recombination rate, it is reasonable to propose that the electronic factor for this process is increased in the mutant through a superexchange mechanism. It has been suggested that electronic coupling between $P^+BPh_L^-$ and the ground state in wt RCs can be enhanced by quantum-mechanical mixing of $P^+BPh_L^-$ with a virtual state such as $P^+BChl_L^-$ or $BChl_L{}^+BPh_L^-$ (*28*). Since the mixing between two states depends inversely on their energy separation, the smaller free energy gap between $P^+\beta_L^-$ and $P^+BChl_L^-$ in (M)L214H RCs would increase the rate of deactivation to the ground state. This interpretation also may explain the effect of a transmembrane electric field on the delayed fluorescence from wt chromatophores (*32*). The proposed mixing of $P^+\beta_L^-$ with a state such as $P^+BChl_L^-$ is quantum mechanical and not thermal in nature, since measurements on (M)L214H RCs at 5 K indicate that the inherent time constant of $P^+\beta_L^-$ charge recombination is about the same (~1 ns) as at 295 K (*33*). An important point is that a greater than tenfold increase in the charge recombination rate is compatible with a much smaller change in the rate of initial electron transfer from P* even if both processes are superexchange-mediated by $P^+BChl_L^-$. This follows because the superexchange energy denominators for for-

ward electron transfer and charge recombination may differ in their sensitivity to ΔG° of $P^+\beta_L^-/P^+BPh_L^-$ because of differences in the shapes and crossing points of the relevant potential energy surfaces (*34*). Additionally, slow structural reorganizations following formation of $P^+\beta_L^-$, as have been proposed to occur in $P^+BPh_L^-$ in wt RCs (*19, 30, 35*), could uncouple the electronic factors for the two processes.

Our results suggest a reason why the native RC may use BPh_L instead of BChl (β_L) as the electron carrier prior to Q_A. Namely, in order to hinder the unwanted charge-recombination process from competing effectively with electron transfer to Q_A, the radical-pair state ($P^+BPh_L^-$ in wt) should lie far enough below $P^+BChl_L^-$ that superexchange-mediated coupling to the ground state is not too large. Similarly, it may be unfavorable for $P^+BChl_L^-$ to lie below P*, since $P^+BChl_L^-$-mediated deactivation of $P^+BPh_L^-$ to the ground state might then be enhanced sufficiently to diminish the quantum yield of charge separation.

The high quantum yield of charge separation depends on an effective competition between electron transfer and charge recombination at each stage of the process. A key insight into RC primary photochemistry is that an optimized Franck-Condon factor for the initial reaction may not simply be associated only with a fast rate, but also with a tolerance toward energetics. Our results also show, however, that raising the energy of $P^+BPh_L^-$ (or $P^+\beta_L^-$) too much can increase the rate of the unwanted charge-recombination reaction of this state, diminishing the yield of electron transfer to Q_A. Thus, highly exothermic deactivation processes in the RC may not be inhibited effectively, due to poor Franck-Condon factors (the inverted region effect), if the electronic coupling is sufficiently large (*12, 24, 25*). These ideas are also exemplified in the heterodimer mutants, in which a BChl of P is changed to BPh (*10–12*), where substantial $BChl^+BPh^-$ intradimer charge-transfer character likely provides an enhanced electronic factor for the ultrafast (~30 ps) deactivation to the ground state, diminishing the yield of electron transfer to BPh_L (*11, 12, 25, 36*). Collectively, these observations argue that a principle means by which the RC achieves a high quantum yield of charge separation is to minimize the participation of states in which charge is separated between strongly interacting chromophores because such states have significant electronic coupling to the ground state.

REFERENCES AND NOTES

1. C. Kirmaier and D. Holten, *Photosynth. Res.* **13**, 225 (1987); D. Budil, P. Gast, C. H. Chang, M. Schiffer, J. R. Norris, *Annu. Rev. Phys. Chem.* **38**, 561 (1987); G. Feher, J. P. Allen, M. Y. Okamura, D. C. Rees, *Nature* **339**, 111 (1989).
2. J. Deisenhofer, O. Epp, K. Miki, R. Huber, H. Michel, *Nature* **318**, 618 (1985); J. P. Allen *et al.*, *Proc. Natl. Acad. Sci. U.S.A.* **83**, 8589 (1986); C. H. Chang *et al.*, *FEBS Lett.* **205**, 82 (1986).
3. T. O. Yeates *et al.*, *Proc. Natl. Acad. Sci. USA* **85**, 7993 (1988).
4. H. Komiya, T. O. Yeates, D. C. Rees, J. P. Allen, G. Feher, *ibid.*, p. 9012.
5. The codon corresponding to position 214 on the M polypeptide was changed from dCTG (Leu) to dCAC (His). This and other procedures are described in V. Nagarajan, W. W. Parson, D. Gaul, C. Schenck, *Proc. Natl. Acad. Sci. U.S.A.* **87**, 7888 (1990). WS8 is a prototrophic strain of *Rhodobacter sphaeroides* described in W. R. Sistrom, *J. Bacteriol.* **131**, 526 (1977).
6. In order for the ground- and transient-state spectra to be consistent with BPh_L remaining in the RC, the new His(M214) residue positioned over BPh_L would need to have the same effect on the Q_X band (an ~1800 cm^{-1} shift to 600 nm) as does a His coordinated to the central Mg^{2+} ion of BChl. This shift would be unprecedented and is not consistent with known metal, ligand, and solvent effects on the visible bands of these and related chromophores. The Q_X band of BPh in a variety of protic and aprotic solvents lies in the narrow range 520 to 540 nm [see (*7, 8*), and P. M. Callahan and T. M. Cotton, *J. Am. Chem. Soc.* **109**, 7001 (1987)]. The position of the Q bands of free base protoporphyrin incorporated into the His-containing heme binding site of proteins such as hemoglobin have essentially the same positions as found in organic solvents [see E. Breslow, R. Koehler, A. W. Girotti, *J. Biol. Chem.* **242**, 4149 (1967); E. D. Sebring and J. Steinhardt, *ibid.* **245**, 5395 (1970)].
7. J. Fajer, D. C. Brune, M. S. Davis, A. Forman, L. D. Spaulding, *Proc. Natl. Acad. Sci. U.S.A.* **72**, 4956 (1975).
8. S. C. Straley, W. W. Parson, D. C. Mauzerall, R. K. Clayton, *Biochim. Biophys. Acta* **305**, 597 (1973); M. van der Rest and G. Gingras, *J. Biol. Chem.* **249**, 6446 (1974).
9. A. Chirino *et al.*, manuscript in preparation.
10. E. J. Bylina and D. C. Youvan, *Proc. Natl. Acad. Sci. U.S.A.* **85**, 7226 (1988).
11. C. Kirmaier, D. Holten, E. J. Bylina, D. C. Youvan, *ibid.*, p. 7562.
12. L. M. McDowell, D. Gaul, C. Kirmaier, D. Holten, C. C. Schenck, manuscript in preparation.
13. The early time course of the photochemistry (initial excitation of P through $P^+Q_A^-$ formation) was investigated on a transient absorption spectrometer having ~150-fs pulses (*11*). Typically 20 to 30% of the RCs were excited. Excitation at 870 nm was used except when probing at wavelengths ≥840 nm, in which case 580-nm excitation was used. (Data from 800 to 840 nm acquired with both excitation wavelengths were used for normalization to obtain the complete spectra in Fig. 3.) Group velocity dispersion in the probe pulse gives a temporal span of <1 ps across the spectra of Figs. 3 to 5. This does not significantly affect the shapes of the spectra and is explicitly taken into account in analysis of the kinetics at each wavelength.
14. The $P^+Q_A^-$ lifetime was measured on an apparatus in which 10-ns excitation flashes at 532 nm were used. The 2 μM samples contained ~20 μM terbutryn to block electron transfer from Q_A to Q_B. The charge-recombination lifetimes at 295 K were 131 ± 3 ms for (M)L214H RCs and 121 ± 3 ms for wt RCs.
15. T. M. Cotton and R. P. Van Duyne, *J. Am. Chem. Soc.* **101**, 7605 (1979).
16. W. W. Parson, R. K. Clayton, R. J. Cogdell, *Biochim. Biophys. Acta* **387**, 265 (1975); V. A. Shuvalov and W. W. Parson, *Proc. Natl. Acad. Sci. U.S.A.* **78**, 957 (1981).
17. When 3 mM solutions of (M)L214H RCs in sodium dithionite are made to reduce Q_A, $P^+\beta_L^-$ has a lifetime of 830 ± 40 ps and ≤5% of the initial amplitude of P-band bleaching remains at 10 ns. This measurement also demonstrates that the 40% decay of P bleaching observed at moderate redox potential is not due to the presence of Q-depleted RCs in the samples.
18. Delayed fluorescence from P* was measured by time-correlated single photon counting on an apparatus in which 1- to 10-pJ, 70- to 80-ps excitation pulses from a laser diode were used (R. DeBey and C. C. Schenck, unpublished results). Numerical deconvolutions and calculation of the molecular free energy ($-\Delta G^\circ$) for the P* → radical pair reaction from the initial amplitude of the major delayed component were performed as described previously (*19*).
19. C. C. Schenck, R. E. Blankenship, W. W. Parson, *Biochim. Biophys. Acta* **680**, 44 (1982); N. W. T. Woodbury and W. W. Parson, *ibid.* **767**, 345 (1984).
20. C. Kirmaier and D. Holten, *Proc. Natl. Acad. Sci. U.S.A.* **87**, 3552 (1990).
21. D. J. Lockhart, C. Kirmaier, D. Holten, S. G. Boxer, *J. Phys. Chem.* **94**, 6987 (1990).
22. N. Woodbury, A. K. Taguchi, J. W. Stocker, S. G. Boxer, in *Proceedings of the Feldafing Workshop on the Structure and Function of Bacterial Reaction Centers*, M. E. Michel-Beyerle, Ed. (Springer-Verlag, Berlin, in press).
23. A. Sarai, *Biochim. Biophys. Acta* **589**, 71 (1980); A. Warshel, Z. T. Chu, W. W. Parson, *Science* **246**, 112 (1989); S. Franzen, R. A. Goldstein, S. G. Boxer, *J. Phys. Chem.* **94**, 5135 (1990).
24. M. R. Gunner and P. L. Dutton, *J. Am. Chem. Soc.* **111**, 3400 (1989).
25. L. M. McDowell, C. Kirmaier, D. Holten, *J. Phys. Chem.* in press.
26. The decrease of about a factor of 2 in the initial electron-transfer rate is consistent with a correspondingly small decrease in the Franck-Condon factor, although it is difficult to quantitatively evaluate the origin of such a small change in rate since the mutation may not only affect ΔG° but the electronic factor and λ for the process.
27. N. W. T. Woodbury, M. Becker, D. Middendorf, W. W. Parson, *Biochemistry* **24**, 7516 (1985); J.-L. Martin, J. Breton, A. J. Hoff, A. Migus, A. Antonetti, *Proc. Natl. Acad. Sci. U.S.A.* **83**, 957 (1986); M. R. Wasielewski and D. M. Tiede, *FEBS Lett.* **204**, 386 (1986); J. Breton, J.-L. Martin, G. R. Fleming, J.-C. Lambry, *Biochemistry* **27**, 8276 (1988); C. Kirmaier and D. Holten *FEBS Lett.* **239**, 211 (1988); D. J. Lockhart, R. F. Goldstein, S. G. Boxer, *J. Phys. Chem.* **89**, 1408 (1988); W. Holzapfel *et al.*, *Chem. Phys. Lett.* **160**, 1 (1989); *Proc. Natl. Acad. Sci. U.S.A.* **87**, 5168 (1990).
28. A. Warshel, S. Creighton, W. W. Parson, *J. Phys. Chem.* **94**, 2696 (1988).
29. P. O. J. Scherer and S. F. Fischer, *Chem. Phys.* **131**, 115 (1989); R. A. Marcus, *Chem. Phys. Lett.* **146**, 13 (1988); R. A. Friesner and Y. Won, *Biochim. Biophys. Acta* **977**, 99 (1989); Y. Hu and S. Mukamel, *Chem. Phys. Lett.* **160**, 410 (1989); A. Warshel, Z.-T. Chu, W. W. Parson, *Biochim. Biophys. Acta* **1017**, 251 (1990).
30. M. Bixon, J. Jortner, M. E. Michel-Beyerle, A. Ogrodnik, *Biochim. Biophys. Acta* **977**, 273 (1989).
31. M. Bixon, J. Jortner, M. E. Michel-Beyerle, *ibid.*, in press.
32. A. Yu. Borisov, V. I. Godik, E. A. Kotova, V. D. Samuilov, *FEBS Lett.* **119**, 121 (1980); E. A. Kotova *et al.*, *ibid.* **131**, 51 (1981).
33. At 5 K the $P^+\beta_L^-$ lifetime is ~800 ps and the $P^+Q_A^-$ yield is ~25%. These correspond to an inherent time constant for deactivation to the ground state of 1.1 ns and inherent time constant for electron transfer to Q_A of 3.2 ns. The latter is thus an activated process.
34. State $P^+BPh_L^-/P^+\beta_L^-$ would cross high on a ground-state surface that is steep since high-frequency modes are the most effective in highly exothermic (1.2 to 1.3 eV) deactivation processes, while $P^+BPh_L^-/P^+\beta_L^-$ would cross near the minimum in the P* surface, which also may be relatively shallow.
35. R. A. Goldstein and S. G. Boxer, *Biochim. Biophys. Acta* **977**, 78 (1989).
36. C. Kirmaier, E. J. Bylina, D. C. Youvan, D. Holten, *Chem. Phys. Lett.* **159**, 251 (1989); L. M. McDowell, C. Kirmaier, D. Holten, *Biochim. Biophys. Acta* **1020**, 239 (1990).
37. R. H. Wendt and V. A. Fassel, *Anal. Chem.* **37**, 920 (1965).

38. C.C.S. gratefully acknowledges support from

USPHS FIRST (GM38214) and Research Career Development (GM00536) Awards and ACS-PRF grant (GM18650). This work was also supported by grant DMB-8903924 from the National Science Foundation (D.H.). D.G. is an NSF Plant Biology Postdoctoral Fellow. Oligonucleotides were synthesized at Colorado State on equipment purchased under NIH grant GM41179. We thank D. Bocian, S. Boxer, R. Friesner, and A. Warshel for stimulating discussions and R. Neumann for preparing RCs.

31 July 1990; accepted 4 December 1990

Chemical Sensors Based on Controlled-Release Polymer Systems

STEVEN M. BARNARD AND DAVID R. WALT*

A novel chemical sensor has been developed in which the polymer ethylene–vinyl acetate is used as a controlled-release system to deliver reagents to the sensing region of an optical fiber for a homogeneous competitive immunoassay based on fluorescence energy transfer. A competition reaction is used to enable continuous measurements of the solution antigen concentration. More generally, the technique allows irreversible indicating chemistries to be used in the construction of chemical sensors that can measure continuously for long periods. Although the sensor configuration has not been optimized in all respects, data are presented for a model system in which a fluorescein-labeled antibody and Texas Red–labeled immunoglobulin G (IgG) are used.

IN THE LAST DECADE, CHEMICAL SENsors have emerged as viable alternatives to traditional methods of analysis. The ideal sensor provides in situ measurements continuously, reversibly, and in real time. The development of a sensor for a particular species depends on the availability of reversible transduction schemes to detect the analyte of interest. Most reversible schemes are based on changes that occur when a chemical compound or membrane interacts with the analyte. The measured properties might be optical or electrical signals, depending on the type of sensor (*1*). In the absence of reversible schemes, irreversible chemistries can be used, such as antibody-based immunoassays, that consume analyte by forming very tight binding complexes with the analyte. These schemes can be used to perform assays or may be used to construct probes, which, by definition, are irreversible and cannot make continuous measurements. However, probes can be adapted to make rapid sequential measurements if reagents are replenished or regenerated. Such probes use pumps to deliver fresh reagent continuously (*2*) or chaotropic reagents to regenerate the binding site of an antibody (*3*). This approach solves some of the problems associated with discrete sampling but does not allow long-term monitoring or true continuous measurements.

To expand the diversity of chemical sensors, we have developed a technique that circumvents the irreversibility of immunoassays and allows us to exploit the specificity and selectivity of antibodies while still preserving continuous measurement capability. To do so, we have adapted a controlled-release delivery system, capable of sustaining a constant release of fresh immunochemicals or any reagent of an irreversible transduction scheme, to perform continuous measurements. Typically, controlled-release systems are biocompatible polymers that release on contact with an aqueous environment by passive diffusion from the polymer matrix [such as ethylene vinyl acetate (*4*)] or hydrolytic breakdown of the polymer structure [such as poly(glycolic acid) (*5*)]. We present preliminary data demonstrating the viability of this idea.

With the advent of hybridoma technology (*6*), it became possible to produce antibodies to virtually any compound. Although the binding between an antibody and antigen is reversible and noncovalent, most immunochemical reactions essentially are irreversible because of the large association constants (K_a), which typically range between 10^5 to 10^9 M^{-1} (*7*). The association constants are composed of large forward (k_1) and small reverse (k_{-1}) rates, ranging from 10^7 to 10^9 M^{-1} s^{-1} and 10^2 to 10^{-4} s^{-1}, respectively. These kinetic parameters make antibodies extremely specific and selective for the analyte of interest.

Fluoroimmunoassays have been developed (*8*) for various proteins (such as antibodies and enzymes), hormones (such as steroids and thyroxine), and drugs (such as digoxin and gentamicin). Immunoassays used clinically fall into two categories. Heterogeneous assays require periods of incubation and washing, while homogeneous assays need no separation step, being based typically on a competition reaction between a fluorescently labeled and an unlabeled antigen (*9*).

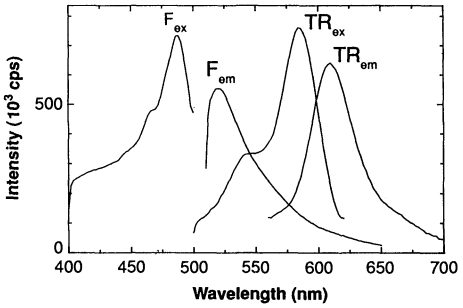

Fig. 1. Excitation and emission spectra of F-Ab to IgG and Texas Red–labeled IgG antigen, showing the overlap of the F-Ab emission spectrum and TR-Ag excitation spectrum.

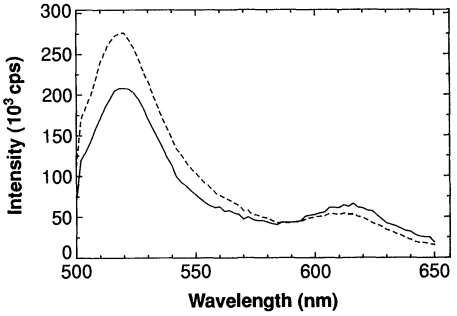

Fig. 2. The dependence of the emission spectra on antigen concentration: spectrum 1 (– – –) high concentration (500 μg/ml); spectrum 2 (——) low concentration (0 μg/ml).

The competitive fluorimmunoassay that we adapted to a controlled-release system is based on a fluorescence energy-transfer mechanism (*10*). When the immunocomplex (F-Ab:TR-Ag) forms between fluorescein-labeled antibody (F-Ab) and Texas Red–labeled IgG (TR-Ag) (Eq. 1)

$$\text{F-Ab} + \text{TR-Ag} \rightarrow \text{F-Ab:TR-Ag} \quad (1)$$

$$\text{F-Ab} + \text{Ag} \rightarrow \text{F-Ab:Ag} \quad (2)$$

the fluorophors are within the critical distance of 10 nm required for nonradiative energy transfer to occur (*11*). Upon excitation, fluorescein molecules transfer their energy to Texas Red nonradiatively, thereby quenching the fluorescein and enhancing the Texas Red intensities. This fluorophor combination was chosen because of the moderately efficient overlap between the emission spectrum of the energy donor, fluorescein, and the excitation spectrum of the energy acceptor, Texas Red, while allowing sufficient resolution of the Texas Red emission peak (Fig. 1). In addition, the dyes are commercially available in reactive forms readily conjugated to proteins (Molecular Probes, Eugene, OR) and have been used in

Max Tishler Laboratory for Organic Chemistry, Department of Chemistry, Tufts University, Medford, MA 02155.

*To whom correspondence should be addressed.